Diffraction efficiency of stepped gratings using high phase-modulation spatial light modulators

Ignacio Moreno,[1,*] Benjamin K. Gutierrez,[2] María M. Sánchez-López,[3] Jeffrey A. Davis,[2] Himkala P. Khanal,[2] and Don M. Cottrell[2]

1. Departamento de Ciencia de Materiales, Óptica y Tecnología Electrónica, Universidad Miguel Hernández de Elche, 03202 Elche, Spain
2. Department of Physics, San Diego State University, San Diego, California 92182-1233, USA
3. Instituto de Bioingeniería, Universidad Miguel Hernández de Elche, 03202 Elche, Spain

Abstract

When encoding diffractive optical elements (DOE) onto a spatial light modulator (SLM), the diffraction efficiency can be reduced because of the pixel nature of the SLM. These effects have been studied previously with displays having the standard phase depth of 2π radians. In this work we explore such effects with devices having a phase-dynamic range as large as 10π. We analyze the quantization effects when displaying blazed phase diffraction gratings in such devices. Experimental results are included where the number of discrete steps per period of the grating as well as the phase modulation depth is varied. Experimental results agree with theory

1. INTRODUCTION

The great advances achieved by the liquid-crystal technology [1] results nowadays in modern spatial light modulators (SLM), with 2D pixelated arrays with about thousands of pixels and pixel dimensions about a few microns. This high resolution motivated the SLM use of optical processing, pioneered in [2], is now generalized and SLMs are used routinely to display dynamic diffractive optical elements (DOE) in all types of applications [3].

A key parameter for the correct and successful use of SLMs is the diffraction efficiency (DE). DE can be reduced by different sources of degradation of the displayed optical function. First, the SLM pixelated structure creates spurious diffraction orders [4]. However, in recent years, this improved dramatically thanks to the improvements of the fill factor (ratio between the pixel size and pixel pitch) achieved in modern liquid-crystal on silicon (LCoS) displays [5]. Other sources of DE degradation that may be present in SLMs are flickering [6], that causes a phase fluctuation effect, and fringing-field effect [7], which becomes more relevant as the pixel size is reduced.

Another source of DE reduction is the complex modulation provided by the SLM. Any deviation from a perfect continuous and linear phase-only modulation with 2π modulation depth results in a DE reduction [8]. In fact, the efficiency reduction caused by a limited phase modulation depth was exploited to design a technique to encode amplitude information onto a phase grating [9].

In this work we analyze DE in terms of the number of phase steps (quantization levels). This subject has been extensively studied in the cases where the maximum phase depth is 2π [10-12]. However, we found more interesting behavior for these cases where the phase depth is

larger. Multi-order diffractive lenses showing various cycles of 2π radians were studied due to their special spectral properties [13]. More recently the use of SLMs with such large phase modulation is becoming of great interest since it allows operating the DOE in higher harmonic orders [14]. This is very interesting to create uncommon spectral properties in diffraction gratings [15] and diffractive lenses [16]. Other uses of SLMs showing such large phase modulation have been demonstrated such as color computer generated holograms [17] or color displays [18]. In addition, large phase modulation can be used also to compensate for fringing effects in SLMs, and therefore **to** reduce pixel crosstalk [19].

Very recently, we demonstrated that an SLM operating in such large modulation range can be used to surpass the classical resolution limit of diffractive lenses encoded onto pixelated devices. Highly efficient lenses with focal lengths much shorter than the classical Nyquist focal length limit were demonstrated [20]. However, this advance showed a requirement to further study the effects of phase quantization levels when this very large phase modulation regime is achieved. Thus, this is the goal of the present work. Here we use phase blazed diffraction gratings and analyze the DE in terms of the number of quantization levels and in terms of the maximum phase modulation range. We find some interesting situations when the number of phase levels is small, and the maximum phase modulation is large. This study is convenient for analyzing the imaging properties of diffractive lenses encoded in this way and defining a new Nyquist limit. The theoretical analysis is accompanied with experimental results that validate the theory, obtained with a LCoS-SLM device designed to operate at the near infrared (NIR) range, but operated at the visible wavelengths where it shows a phase modulation range up to 10π radians for a wavelength of 458 nm.

2. REVIEW OF THE FOURIER TRANSFORM ANALYSIS OF STEPPED GRATINGS

We begin by analyzing the Fourier transform of a blazed phase stepped grating with a number N of equidistant phase steps, and a maximum phase depth of $M2\pi$ radians. Figure 1 illustrates the phase profile, where d indicates the grating's period. Note that each phase step has a width of d/N and the phases take values 0, β, 2β, 3β … $(N\text{-}1)\beta$, where $\beta = M2\pi/N$ denotes the phase jump at each step.

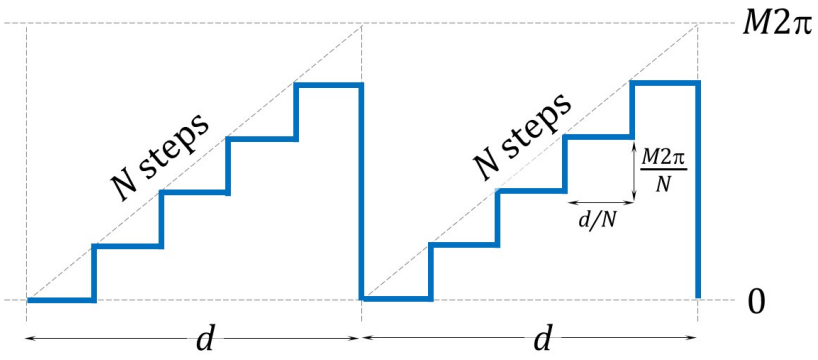

Fig. 1. Phase profile of a blazed phase stepped grating with period d, maximum phase depth $M2\pi$ and N steps.

The Fourier series coefficient of this stepped phase grating is given by:

$$c_\alpha = \frac{1}{d}\sum_{n=0}^{N-1}\left(\int_{nd/N}^{(n+1)d/N} e^{-iM2\pi n/N} e^{i\alpha 2\pi x/d} dx\right). \quad (1)$$

It is a straightforward calculation [11] to derive these coefficients, which are given by

$$c_\alpha = e^{i\frac{\pi\alpha}{N}} \frac{e^{-i\pi(M-\alpha)}}{e^{-i\frac{\pi}{N}(M-\alpha)}} \cdot \frac{\sin\left(\frac{\pi\alpha}{N}\right)}{\pi\alpha} \cdot \frac{\sin(\pi(M-\alpha))}{\sin\left(\frac{\pi}{N}(M-\alpha\right)}. \quad (2)$$

Therefore, the relative efficiency at each diffraction order is given by:

$$\eta_\alpha(M,N) = |c_\alpha|^2 = \left(\frac{\sin\left(\frac{\pi\alpha}{N}\right)}{\pi\alpha}\right)^2 \left(\frac{\sin(\pi(M-\alpha))}{\sin\left(\frac{\pi}{N}(M-\alpha)\right)}\right)^2. \quad (3)$$

We consider two limiting cases of this general situation:

2.1 Case without quantization

In this case for a continuous phase grating the limit $N\to\infty$ is considered, resulting in

$$\eta_\alpha(M) = \left(\frac{\sin(\pi(M-\alpha))}{\pi(M-\alpha)}\right)^2 = \mathrm{sinc}^2(M-\alpha). \quad (4)$$

where $\mathrm{sinc}(x)=\sin(\pi x)/(\pi x)$. For $M=0$, all the energy starts at the zero order. However, as the phase depth varies in the range $0<M<1$ the energy splits into the zero and first orders and is entirely in the first order when M=1. This is the situation that was exploited to encode amplitude in the technique in [8].

When the maximum phase modulation depth increases even more, the energy in the first order decreases while now is the second order which increases, reaching the maximum efficiency when $M=2$ [14]. If the maximum modulation continues increasing, thus having larger values of M, the energy is mainly distributed among the diffraction orders $\alpha=\mathrm{int}(M)$ and $\alpha=\mathrm{int}(M+1)$, where $\mathrm{int}(M)$ denotes the integer part of M. When M is a semi-integer the energy splits into two equally intense orders $\alpha=\mathrm{int}(M)$ and $\alpha=\mathrm{int}(M+1)$. And when M is an integer, all the energy is diffracted on to the diffraction order $\alpha=M$. Figure 2(a) illustrates this energy transfer between successive orders as the value of M increases.

2.2 Case with 2π phase modulation ($M=1$)

This is the case where a stepped diffraction grating with N phase levels distributed along the 2π modulation range are considered. In this case $M=1$ and the general equation (3) adopts the result

$$\eta_\alpha(N) = \left(\frac{\sin\left(\frac{\pi\alpha}{N}\right)}{\pi\alpha}\right)^2 \left(\frac{\sin(\pi(1-\alpha))}{\sin\left(\frac{\pi}{N}(1-\alpha)\right)}\right)^2. \quad (5)$$

When the order $\alpha=1$ is considered, the classical relation for the diffraction efficiency [10] is retrieved

$$\eta_1 = \left(\frac{\sin\left(\frac{\pi}{N}\right)}{\pi/N}\right)^2 = \mathrm{sinc}^2\left(\frac{1}{N}\right). \quad (6)$$

Figure 2(b) represents this classical relation of η_1 versus N. When $N = 2$ (binary phase grating), the efficiency at the first order is about 40.5%, it is about 68.4% for $N = 3$ levels, and it reaches more than 91% with only $N = 6$ levels.

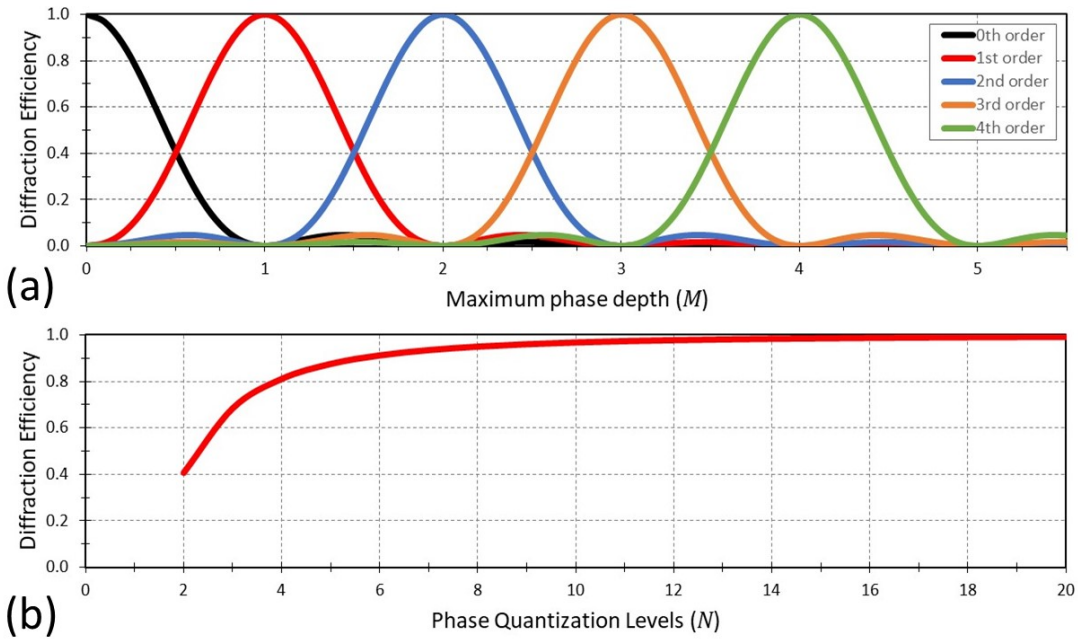

Fig. 2. Diffraction efficiency in two limits: (a) η_α versus M for orders α=0,1,2,3,4 in case there is no quantization ($N\to\infty$) (b) η_1 versus the number N of phase quantization levels for the standard case M=1.

Before discussing other results, we will discuss our experimental setup. That will allow us to examine the agreement between theory and experiment in a more convenient way.

3. EXPERIMENTAL SETUP AND RESULTS

3.1 Experimental system

Both universities participating in this work have developed equivalent setups shown in Fig. 3(a). We used either an argon ion laser (blue line at the wavelength of 458 nm) or a collimated green laser-diode-pumped DPSS laser module from Thorlabs (model CPS520, with a wavelength of 520 nm). The laser beam passes through a spatial filter and a collimating lens and is sent through a 1" non-polarizing beamsplitter (NPBS) to a reflective LCoS-SLM device. A linear polarizer selects the polarization component parallel to the LCoS director. The light is reflected by the LCoS device, and passes again through the NPBS to a detector. The system is rather compact.

We used a Hamamatsu LCoS device (model X10468-08) designed for use in the 1000-1500 nm range for telecommunication applications. This series of devices are characterized by displays of 792×600 pixels with a pixel spacing of Δ=20 μm. The device was calibrated by placing it between crossed or parallel polarizers and studying the reflection as a function of gray level [21]. The LCoS device provides a phase modulation depth up to 8π when using the green wavelength of 520 nm, where the gray level supplied by the computer controls the phase level. And for the

blue wavelength of 458 nm of the argon laser it is even larger, reaching a maximum phase of 10π [20]. A phase difference of 2π is achieved approximately every 64 gray levels for the wavelength of 520 nm, and every 50 gray levels for the wavelength of 458 nm. Therefore, this device allows reaching values M=1, 2, 3, 4, and even 5 for these wavelengths.

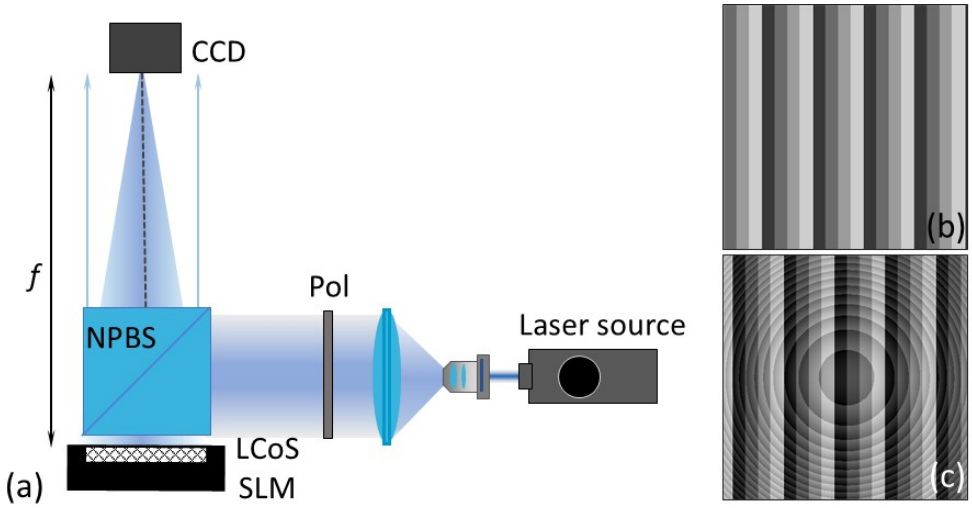

Fig. 3. (a) Scheme of the optical setup. Images addressed to the LCoS SLM to generate (b) A stepped blazed grating grating with N=4; (c) The same grating plus the focusing lens.

Blazed diffraction gratings have been programmed with different values of M and N in order to analyze the diffraction efficiency in these cases. In all cases a period of 60 pixels was selected. This large value was selected to stay far from the resolution limit and avoid overlapping with secondary orders generated by the pixelated structure of the device [22]. It also prevents the measurements to be affected by pixel crosstalk due to fringing effect, which is much stronger for small periods [19].

Since the LCoS device is not designed to operate at the visible wavelengths, a significant portion of the input beam is reflected by the optical coating and is not being modulated by the device, thus contributing additionally to the zero-order component. In order to avoid this additional effect, the phase function of a lens was added to the phase function of the grating. This way, the lens encoded on the SLM focuses the diffracted orders generated by the encoded grating (instead of using a physical external lens to focus them). The light reflected from the optical coating is not affected by the lens encoded on the SLM and therefore remains as an unfocused plane wave that simply adds a slight background to the diffraction orders.

The grating and lens patterns are formed on a 1024×1024 array and overfill the LCoS screen. The encoded lens has a focal length of f=75 cm, much larger than the effective Nyquist limit given by f_N=52.4 mm for 458 nm or f_N=46.1 mm for 520 nm [20]. Figure 3(b) shows, as an example, the central area of the image addressed to the display to generate the stepped blazed grating with N=4 steps. And Fig. 3(c) shows the corresponding image when the lens is added to the grating. The lens is encoded using 50 or 64 gray levels, so it operates as a standard blazed diffractive lens with M=1.

For most of the experiments, we used a Basler camera (model acA1300-200um) to record the intensities of the diffracted peaks in the Fourier plane of the encoded lens function. This camera has 1280x1024 pixels having a size of 4.8 μm. It uses a Pylon Viewer software that allows to directly obtain quantitative measurements of the intensity.

Next, we compare theoretical predictions with experimental results. In most of the experiments we use the wavelength of 520 nm, and we select three different modulation regimes corresponding to M=1, 2, and 3 (maximum phase depth of 2π, 4π and 6π). A remaining 2π phase modulation is left to encode the lens. For each case the diffraction pattern is captured for a number of levels from N=2 up to 16. The captures show orders from α=-5 to α=+5.

3.2 Standard case with 2π phase modulation (M=1)

We first review the case where the modulation depth is 2π corresponding to M=1. Figures 4(a) to 4(d) show the expected relative intensity of each diffraction order as N increases. For each case, on the right, a profile of the phase function in one period is drawn. It is interesting to note how the most intense diffraction orders after the target order α=1 are those with α=1±N.

Experimental results are shown in Fig. 4(e) for this case and experimental results agree with the theory.

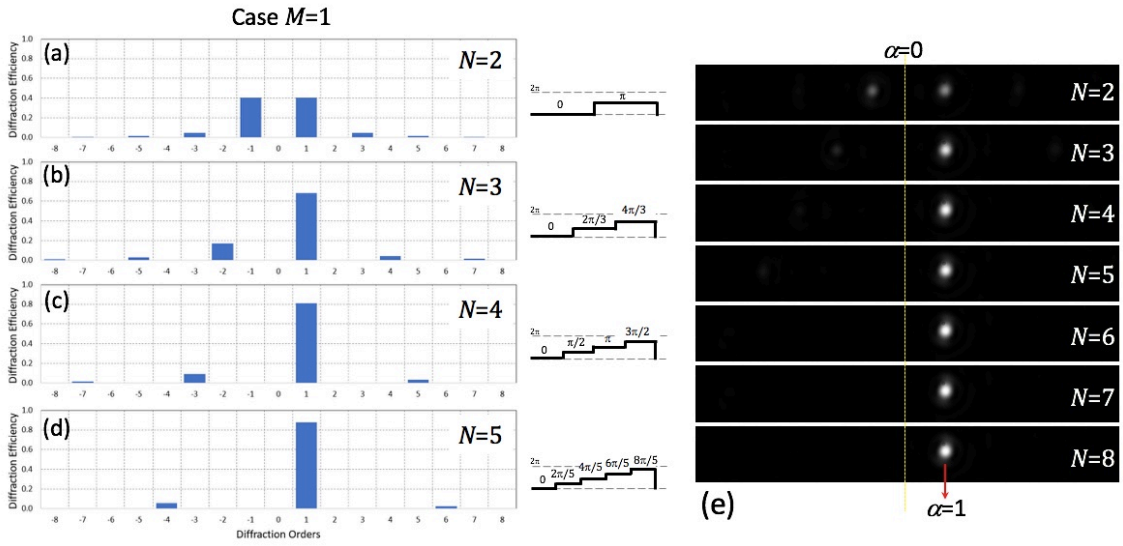

Fig. 4. (a)-(d) Expected relative intensity of diffraction orders versus the number N of phase quantization levels for the standard case M=1. The phase profile in one period is drawn for each case. (e) Corresponding experimental results.

4. DIFFRACTION EFFICIENCY FOR LOW QUANTIZATION LEVELS AND LARGE PHASE MODULATION

In this section we explore some interesting intermediate cases, derived from the general Equation (3) that occur when a small number N of quantization levels are considered combined with large phase modulation values of M.

A first important point to note is that when the number of phase quantization levels is N=$2M$, then each phase step is of π radians. Therefore, the phase grating becomes equivalent to a binary phase grating with π phase shift, and most of the energy (81%) is split in two symmetric diffraction orders, each one receiving 40.5% of the energy. In the standard case when M=1, this happens for the minimum possible value N=2, shown in the first graph of Fig. 4.

However, for larger values of M the binary phase grating is reproduced with larger N, and very interesting effects are produced when N is decreased even more, N<$2M$.

4.1 Case with M=2

A first example of this situation is shown in Fig. 5, which corresponds to the case M=2 (maximum phase shift of 4π). We first note the pattern when N=2 is considered (Fig. 5(a)). In this situation, the two levels have phases 0 and 2π respectively, i.e., there is no phase difference between the two levels. As a consequence, all the energy is focused on the zeroth diffraction order.

A second much more interesting case happens for N=3 (Fig. 5(b)). Interestingly the most intense order is now α=-1, with a relative intensity of 68.4%. This "opposite" diffraction can be easily understood by looking at the grating phase profile drawn in the figure. The three phase levels take values of 0, $4\pi/3$ and $8\pi/3$. By subtracting multiples of 2π equivalent phase values can be obtained and the grating's profile can be regarded equivalent to having phases 0, $-2\pi/3$ and $-4\pi/3$. Note that this is equivalent to the standard case of N=3 shown in Fig. 4 (M=1) but oriented in the opposite direction, thus diffracting in opposite angle. This effect was noticed many years ago and proposed to diffract different colors in opposite angles [22].

The diffraction pattern when M=2 and N=4 is considered in Fig. 5(c) and reproduces the binary phase grating. Now the phase steps take values of 0, π, 2π and 3π. After considering modulo 2π, this is equivalent to a binary π-phase grating, but with half the period with respect to the original grating. This is the reason why the two most intense diffraction orders (with the efficiencies of 40.5%) are now α=±2. The next more intense orders are at α=±6.

If the number N continues increasing, then the energy starts to concentrate on the order α=+2, as expected from the result without quantization described in Fig. 2(a). For N=5 the phase steps are of $4\pi/5$ (Fig. 5(d)). The phase profile after considering modulo 2π results in a phase profile that resembles those of the non-synchronously sampled gratings analyzed in [24].

For N=6 the phase steps are of $2\pi/3$ (Fig. 5(e)). The phase profile after modulo 2π results in the standard blazed grating with M=1 and only N=3, but with half the period. Therefore, the same pattern shown in Fig. 4(b) (case N=3) is now reproduced in Fig. 5(e) (case N=6) but located at diffraction orders with twice the indices α.

It is also interesting to note in the last two cases in Figs. 5(d) and 5(e) how the most intense orders, after α=+2, are those with α=2±N. Therefore, as N increases the energy not going to the main diffraction order is splitting further apart to higher harmonic orders.

All the experimental results shown in Fig. 5(f) agree very well with these expected results.

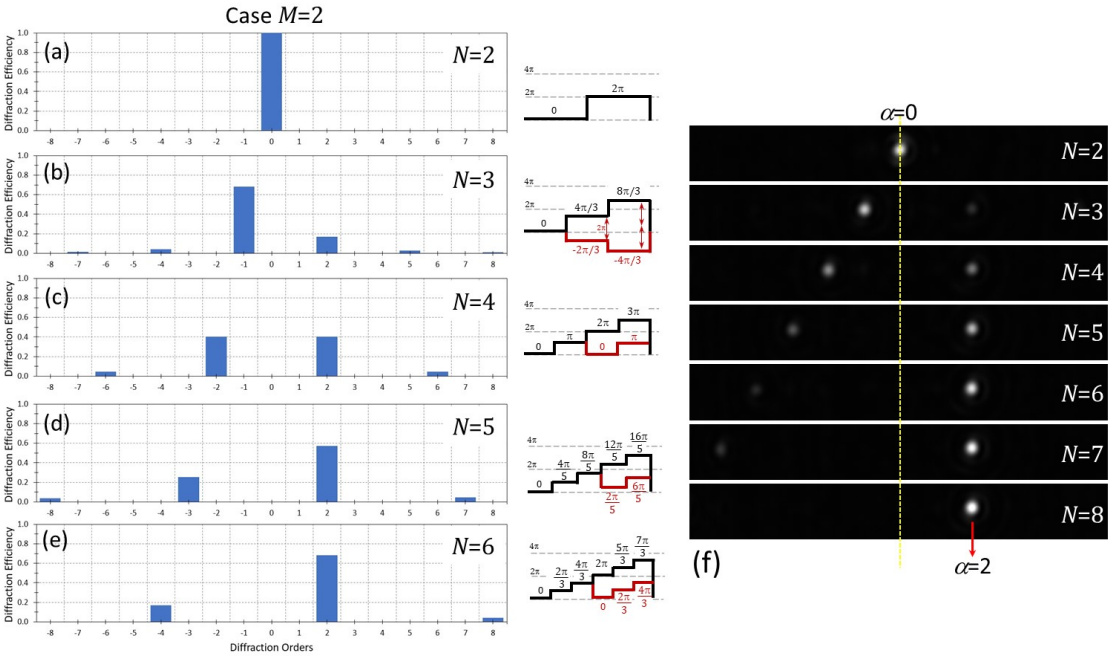

Fig. 5. (a)-(e) Expected relative intensity of diffraction orders versus the number N of phase quantization levels for the case M=2. The phase profile in one period is drawn for each case. (f) Corresponding experimental results.

4.2 Case with M=3

As a second example, Fig. 6 shows equivalent results but now the SLM can reach M=3 (maximum phase shift of 6π). In the first plot, for N=2, now the two levels have phases 0 and 3π respectively, i.e., reproduces a binary π-phase grating, and the diffraction orders α=±1 therefore have equal efficiency of 40.5% (Fig. 6(a)). For N=3 levels, now the phase step is of 2π, and therefore there is no grating, and all the energy is concentrated on the zero order (Fig. 6(b)).

The diffraction pattern becomes interesting for N=4. Now the phase steps are of $3\pi/2$ (Fig. 6(c)). The most intense order is α=−1, with an efficiency about 81%. To understand this pattern, we can again subtract multiples of 2π to the different steps and show that the grating's profile has phase values equivalent to 0, $-\pi/2$, $-\pi$ and $-3\pi/2$. This is equivalent to the standard blazed grating with four levels, but again diffracting in the opposite angle. A similar argument explains the case for N=5, although now the most intense order is α=−2 (Fig. 6(d)). This grating profile again reproduces those of non-synchronously sampled gratings [24].

A transition from "opposite" diffraction to the standard non-stepped case is produced now when N=6. For this case the phase difference between steps is of π and therefore a binary phase profile is again reproduced, now with one third of the original period (Fig. 6(e)). This is why the two orders receiving each 40.5% of the total energy are now α=±3.

After this transition, when N is greater than $2M$ then the energy starts to concentrate on the order α=M, as expected form the limit without quantization. In this case the first value is N=7, as shown in the last graph in Fig. 6(f).

Experimental results shown in Fig. 6(g) again agree very well with all these predictions.

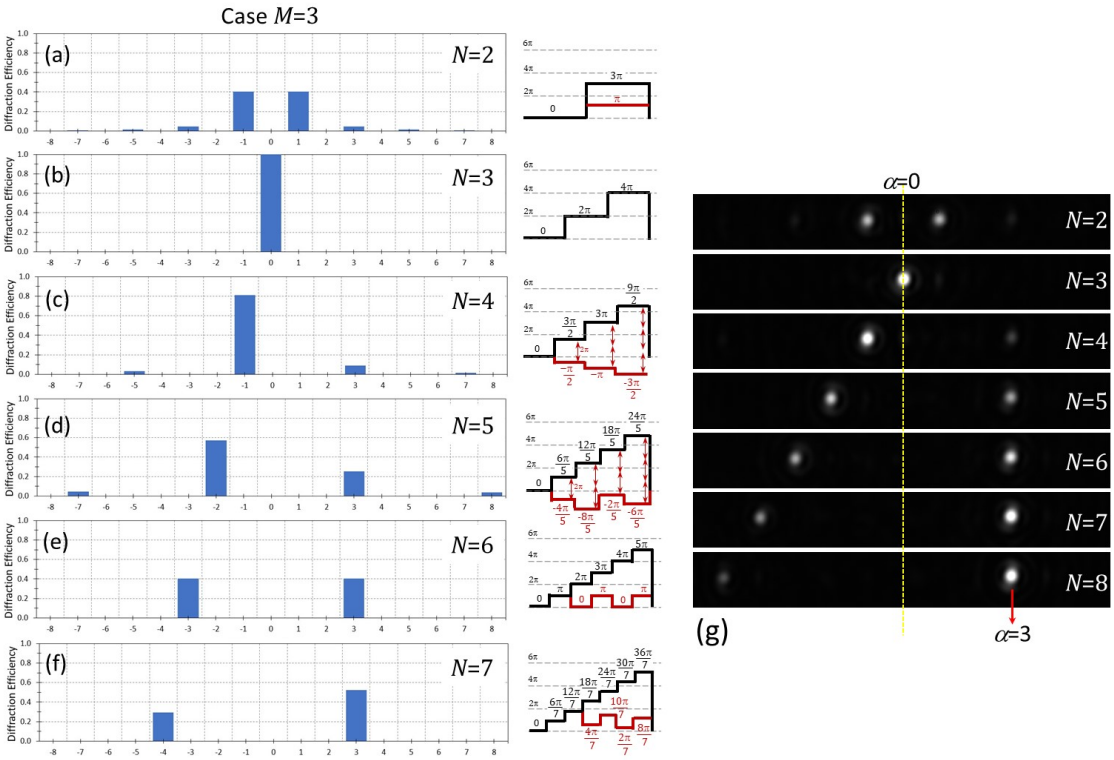

Fig. 6. (a)-(f) Expected relative intensity of diffraction orders versus the number N of phase quantization levels for the case M=3. The phase profile in one period is drawn for each case. (g) Corresponding experimental results.

4.3 Quantitative measurements of diffraction efficiency with the number of steps

In order to quantitively compare the different cases, Fig. 7 shows the diffraction efficiency η_α as a function of the number of steps N, for the diffraction order α=M for cases M=1,2,3,4. The general Eq. (3) that describes the efficiency as a function of N and M, reads as:

$$\eta_{\alpha=M}(M,N) = \left(\frac{\sin\left(\frac{\pi M}{N}\right)}{\frac{\pi M}{N}}\right)^2 = \mathrm{sinc}^2\left(\frac{M}{N}\right), \qquad (7)$$

when the order α=M is considered. This relation thus represents a generalization of the classical law (Eq. (5)) of the standard case M=1 for higher values of M.

The continuous curves in Figs. 7(a) to 7(d) show $\eta_{\alpha=M}$ as a function of N for the cases M=1,2,3 and 4 respectively. They all show an asymptotic tendency to maximum efficiency as N reaches large values. The dots in this figure indicate experimental measurements. These experimental values have been obtained by measuring the intensity at the corresponding diffraction order for gratings with the same period but different values of N. The values are normalized to the intensity measured for a very large value of N (about 60), that can be considered to lead to the maximum efficiency. We remind that we use gratings with a period of 60 pixels. For this value, the encoded stepped gratings show the same number of pixels in each step for cases N=2, 3, 4, 5 and 6. For other values we approximate the transition from one step to the next one by the closest pixel.

In order to quantitatively measure their relative intensities we slightly defocused of the diffraction orders and added the values of the blur spots captured by the camera. The experimental results in Fig. 7 show very good agreement with the theory despite these approximations.

Figure 7(a) shows the standard diffraction efficiency η_1 of the α=+1 diffraction order versus N for M=1. Note that a diffraction efficiency of about 70% is achieved with only N=3 levels. Similarly, Figs. 7(b) and 7(c) show the diffraction efficiencies η_2 and η_3 for M=2 and M=3 respectively. Note that an efficiency of 40.5% (binary phase grating) is achieved for N=2, N=4, N=6 and N=8 in Figs. 7(a), 7(b), 7(c) and 7(d) respectively. Finally, Fig. 7(d) shows that an efficiency of 70% requires N=12 levels.

The results in Fig. 7(d) cannot be obtained directly as the other cases for the wavelength of 520 nm. Since the LCoS-SLM provides only M=4, which are employed to display the grating, we need additional 2π of phase to encode the lens. This can be done with the wavelength of 458 nm. However, it is possible to encode the sum of the M=4 grating with the lens and only use 8π of phase. In the pixels where the phase exceeds 8π we simply subtract 2π. Since we are operating with monochromatic light, this operation provides an equivalent phase function. The experimental results in Fig. 7(d) justify this approach for this example.

All cases in Fig. 7 show that for larger N the energy concentrates in the corresponding order (α=M), in agreement with the limit without quantization shown in Fig. 2(a). However, as the value of M is greater the increase of the efficiency to the corresponding order is slower.

These data show opposite consequences of using these higher modulation levels. On the one hand, we get an enhancement of the phase encoded by the LCoS as shown in Ref. [20], where the focal length of a lens was reduced by a factor of M. On the other hand, the diffraction efficiency is reduced as the number of encoded levels decreases. Our results seem to favor the former advantage. Note that a diffraction efficiency of 70% is achieved for N=3 levels when M=1. On the other hand, the same diffraction efficiency requires N=6 levels when M=2, N=9 pixels when M=3, and N=12 levels when M=4.

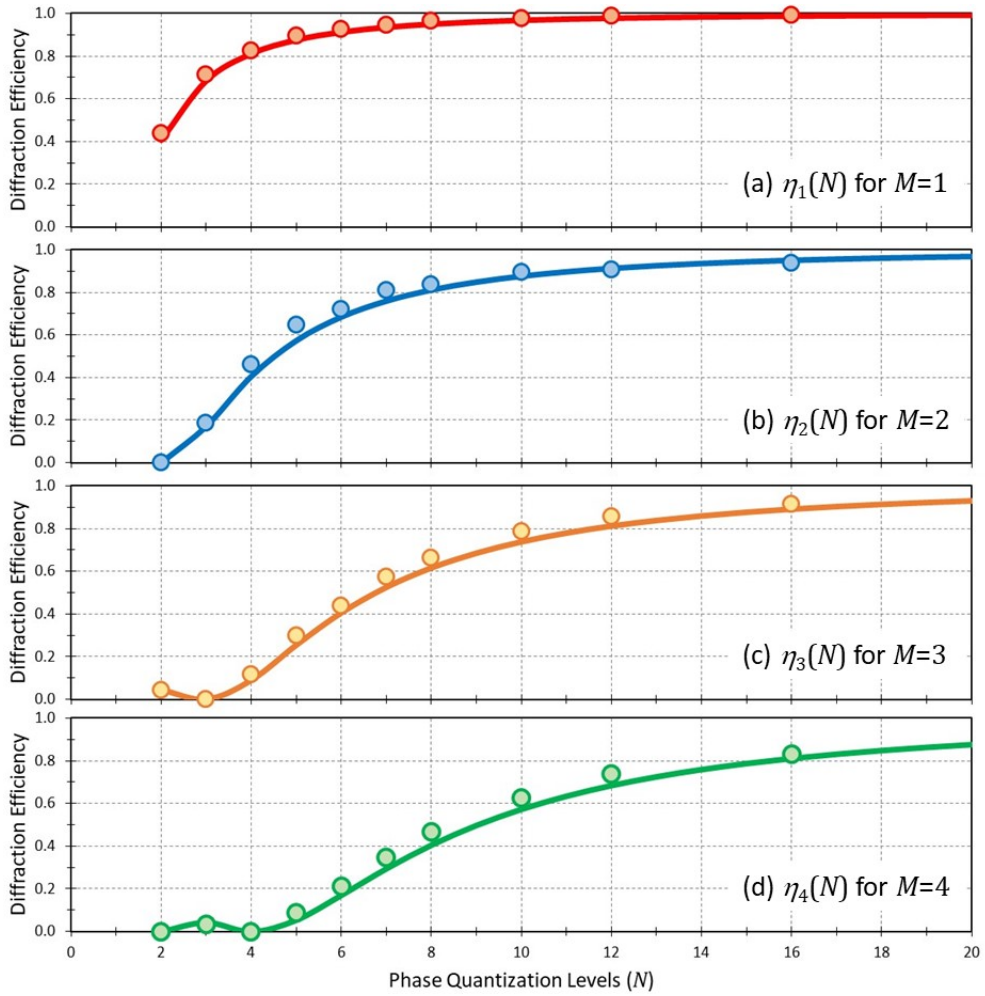

Fig. 7. Diffraction efficiency versus the number *N* of phase quantization levels. (a) η_1 for M=1. (b) η_2 for M=2. (c) η_3 for M=3. (d) η_4 for M=4. Dots indicate experimental measurements.

4. CONCLUSIONS

In summary, this work provides an analysis of the effects of phase quantization in spatial light modulators showing large values of phase modulation range. This study is relevant since such regimes of phase modulation are receiving increasing interest to display diffractive optical elements with novel features. In particular, we recently showed how operating at this large modulation regime can be used to surpass the classical Nyquist resolution limit for the shortest focal length of a diffractive lens that can be encoded in the SLM without being affected by aliasing.

In order to understand the properties of diffractive elements operating at this large phase modulation regime, it is necessary to study the diffraction mechanisms when we approach the resolution limit. In this work we displayed blazed phase gratings but changed the number of phase quantization steps (N) and the maximum phase modulation range ($M2\pi$). The case when the number of phase steps is N=$2M$ is identified as transition. For this case the grating operates as a binary π-phase grating diffracting light mainly to orders α=±M, each one receiving 40.5% of the relative efficiency.

For $N>2M$ the light efficiency concentrates at the diffraction order $\alpha=M$ following the expected tendency to increase the efficiency as the number N increases. Equation (6) represents the generalization to higher values of M of the classical formula in Eq. (3) for the standard case with $M=1$.

Some interesting diffraction phenomena occur when the number of quantization levels is $N<2M$. In this situation, the phase steps in the grating are so big that the grating's blazed phase profile is under-sampled, producing situations where the most intense order is not the expected $\alpha=M$; on the contrary, for some cases the most intense order appears in opposite angle. We have presented equivalent phase profiles by subtracting 2π steps, which explain this behavior.

Finally, we have presented experimental verification of all these effects by using a LCoS-SLM device that shows a phase modulation as large as 8π radians for 520 nm or 10π radians for 458 nm. To achieve this very large phase modulation regime we use a device intended for use in the infrared range, but illuminated with these short visible wavelengths. In order to achieve good results, the SLM encodes simultaneously the grating and a lens that focuses the diffraction pattern onto the detector, while the non-modulated component of the input beam (reflected by the antireflection coating on the device, designed to transmit IR wavelengths) remains unfocused and contributes only to some background weak noise to the diffraction orders pattern.

Similar results were obtained at both wavelengths. We present here the data at 520 nm for this work to remain consistent and because that data is the most recent.

We believe this study is interesting for users of SLMs and can contribute to extend the recent interest in using devices with very large phase modulation. It can be useful also to redefine classical concepts of diffractive optics, like the Nyquist limit of the focal length [20] imposed by the spatial resolution.

Acknowledgements

Ignacio Moreno and María M. Sánchez-López acknowledge funding from Conselleria d'Educació, Investigació, Cultura i Esport; Generalitat Valenciana (PROMETEO-2017-154); and Ministerio de Ciencia, Innovación y Universidades (Ministerio de Ciencia e Innovación (MICINN) (RTI2018-097107-B-C33).

REFERENCES

1. D. K. Yang and S.-T. Wu, *Fundamentals of Liquid Crystal Devices*, 2nd Edt., New York, Wiley (2015).
2. H. K. Liu, J. A. Davis, and R. A. Lilly, "Optical-data-processing properties of a liquid-crystal television spatial light modulator," Opt. Lett. **10**(12), 635–637 (1985).
3. T. Haist and W. Osten, "Holography using pixelated spatial light modulators—part 1: theory and basic considerations," J. Micro/Nanolithogr MEMS MOEMS **14**(4), 041310 (2015).

4. J. A. Davis, J. B. Chambers, B. A. Slovick, and I. Moreno, “Wavelength-dependent diffraction patterns from a liquid crystal display,” Appl. Opt. **47**(24), 4375-4380 (2008).
5. Z. Zhang, Z. You, and D. Chu, "Fundamentals of phase-only liquid crystal on silicon (LCOS) devices", Light Sci. Appl. **3**, e213 (2014).
6. I. Moreno, A. Lizana, A. Márquez, C. Iemmi, E. Fernández, J. Campos, and M. J. Yzuel, “Time fluctuations of the phase modulation in a liquid crystal on silicon display: characterization and effects in diffractive optics,” Opt. Express **16**(21), 16711–16722 (2008).
7. C. Lingel, T. Haist, and W. Osten, “Optimizing the diffraction efficiency of SLM-based holography with respect to the fringing effect,” Appl. Opt. **52**(28), 6877-6883 (2013).
8. J. A. Davis, D. M. Cottrell, J. Campos, M. J. Yzuel, and I. Moreno, “Encoding amplitude information onto phase-only filters,” Appl. Opt. **38**(23), 5004-5013, (1999).
9. I. Moreno, C. Iemmi, A. Márquez, J. Campos, and M. J. Yzuel, “Modulation light efficiency of diffractive lenses displayed in a restricted phase-mostly modulation display,” Appl. Opt. **43**(34), 6278-6284 (2004).
10. G. J. Swanson, W. B. Veldkamp, “Diffractive optical elements for use in infrared systems”, Opt. Eng. **28**(6), 605-608 (1989)
11. I. A. Erteza, “Diffraction efficiency analysis for multi-level diffractive optical elements”, Sandia Report, SAND95-1697, (1995).
12. B. Kress and P. Meyrueis, *Digital Diffractive Optics*, John Wiley & Sons, Chichester, UK (2000).
13. D. Faklis and G. M. Morris, “Spectral properties of multi-order diffractive lenses,” Appl. Opt. **34**(14), 2462-2468 (1995).
14. J. Albero, P. Garcia-Martinez, J. L. Martinez, and I. Moreno, “Second order diffractive optical elements in a spatial light modulator with large phase dynamic range,” Opt. Lasers Eng. **51**(2), 111-115 (2013).
15. V. Calero, P. Garcia-Martinez, J. Albero, M. M. Sanchez-Lopez, and I. Moreno, “Liquid crystal spatial light modulator with very large phase modulation operating in high harmonic orders,” Opt. Lett. **38**(22), 4663-4666 (2013).
16. J. L. Martinez, E. J. Fernandez, P. M. Prieto, P. Artal, “Chromatic aberration control with liquid crystal spatial phase modulators,” Opt. Express **25**(9), 9793-9801 (2017).
17. A. Jesacher, S. Bernet, and M. Ritsch-Marte, “Colour hologram projection with an SLM by exploiting its full phase modulation range,” Opt. Express **22**(17), 20530-20541 (2014).
18. W. Harm, A. Jesacher, G. Thalhammer, S. Bernet, and M. Ritsch-Marte, “How to use a phase-only spatial light modulator as a color display,” Opt. Lett. **40**(4), 581–584 (2015).
19. S. Moser, M. Ritsch-Marte, and G. Thalhammer, “Model-based compensation of pixel crosstalk in liquid crystal spatial light modulators,” Opt. Express. **27**(18), 25046– 25063 (2019).
20. B. K. Gutierrez, J. A. Davis, I. Moreno, and D. M. Cottrell, “Encoding lenses with focal lengths lower than the Nyquist limit using high phase-modulation displays,” Opt. Lett. **44**(13), 3398-3401 (2019).
21. J. A. Davis, P. Tsai, and D. M. Cottrell, “Transmission variations in liquid crystal spatial light modulators caused by interference and diffraction effects,” Opt., Eng. **38**(6), 1051-1057 (1999).

22. J. A. Davis, B. A. Slovick, C. S. Tuvey, and D. M. Cottrell, “High diffraction efficiency from one- and two-dimensional Nyquist frequency binary-phase grating,” Appl. Opt. **47**(15), 2829-2834 (2008).
23. H. Dammann, “Color separation gratings”, Appl. Opt. **17**(15), 2273-2279 (1978).
24. J. A. Davis, J. Adachi, and D. M. Cottrell, “Diffraction efficiency of nonsynchronously sampled diffraction gratings”, Opt. Eng. **41**(11), 2983-2986 (2002).